Journal of Neurotrauma
39:715–723 (May 2022)

DOI: 10.1089/neu.2021.0412

Journal of Neurotrauma

ORIGINAL ARTICLE

Hyperbaric Oxygen Therapy after Mid-Cervical Spinal Contusion Injury

Sara M.F. Turner,[1,2] Michael D. Sunshine,[1–3] Vijayendran Chandran,[4] Ashley J. Smuder,[3,5] and David D. Fuller[1–3,*]

Abstract

Hyperbaric oxygen (HBO) therapy is frequently used to treat peripheral wounds or decompression sickness. Evidence suggests that HBO therapy can provide neuroprotection and has an anti-inflammatory impact after neurological injury, including spinal cord injury (SCI). Our primary purpose was to conduct a genome-wide screening of mRNA expression changes in the injured spinal cord after HBO therapy. An mRNA gene array was used to evaluate samples taken from the contused region of the spinal cord following a lateralized mid-cervical contusion injury in adult female rats. HBO therapy consisted of daily, 1-h sessions (3.0 ATA, 100% O_2) initiated on the day of SCI and continued for 10 days. Gene set enrichment analyses indicated that HBO upregulated genes in pathways associated with electron transport, mitochondrial function, and oxidative phosphorylation, and downregulated genes in pathways associated with inflammation (including cytokines and nuclear factor kappa B [NF-κB]) and apoptotic signaling. In a separate cohort, spinal cord histology was performed to verify whether the HBO treatment impacted neuronal cell counts or inflammatory markers. Compared with untreated rats, there were increased NeuN positive cells in the spinal cord of HBO-treated rats ($p = 0.004$). We conclude that HBO therapy, initiated shortly after SCI and continued for 10 days, can alter the molecular signature of the lesioned spinal cord in a manner consistent with a neuroprotective impact.

Keywords: cervical; gene array; hyperbaric oxygen; spinal cord injury

Introduction

Hyperbaric oxygen (HBO) therapy involves brief (≤ 1 h) exposure to pressurized oxygen at ≤3 ATA and is used frequently to aid peripheral wound healing and to treat decompression sickness.[1] Evidence suggests that HBO provides neuroprotection after central nervous system injury including stroke and spinal cord injury (SCI).[2–4] Neuroprotection is defined as a reduction of the secondary damage that occurs as a result of pathophysiological processes triggered by acute injury.[5] Neuroprotection within the context of SCI could mitigate apoptosis,[6,7] demyelination,[8] and axonal degeneration.[7]

Studies of HBO therapy after SCI date back at least 50 years. Early reports showed that O_2 partial pressure (PO_2) in the acutely injured spinal cord approached 0 mm Hg,[9] but HBO could drive spinal PO_2 near the lesion site to 200–500 mm Hg.[10] Subsequent studies showed that acute HBO therapy after SCI could reduce necrosis and improve motor recovery.[11,12] Recent years have seen an increase in experimental studies of HBO therapy following SCI. Studies in rodent SCI models have reported that HBO can attenuate spinal oxidative stress,[13,14] reduce apoptosis,[15,16] and improve motor recovery.[17–19]

Departments of [1]Physical Therapy, [4]Pediatrics, and [5]Applied Physiology and Kinesiology, and [2]McKnight Brain Institute, and [3]Breathing Research and Therapeutics Center, University of Florida, Gainesville, Florida, USA.

*Address correspondence to: *David D. Fuller, PhD, Department of Physical Therapy, University of Florida, PO Box 100154, Gainesville, FL 32610, USA E-mail:* dfuller@phhp.ufl.edu

Our primary purpose was to conduct a genome-wide screening of mRNA expression changes in the injured spinal cord of adult rats following HBO therapy. Transcriptomics is a highly informative starting point to guide subsequent proteomic, metabolomics, or other experiments. We reasoned that such data would be valuable to the field, and the method also provides an unbiased way to determine if HBO impacts the overall ''genetic signature'' of the injured spinal cord. Based on previous histological studies,[16,20] we hypothesized that following HBO therapy, mRNA gene array and gene set enrichment analysis (GSEA)[21] of the injured spinal cord in adult rats would indicate downregulation of processes associated with neuronal loss and inflammation. The GSEA data were complemented with histological assessment of neuron and inflammatory cell counts, which were performed to validate that HBO impacted the injured spinal cord, as in previous reports.[15,16] Brief, daily HBO therapy was initiated shortly after SCI and continued for 10 days.

Methods

Experimental animals

All procedures were approved by the University of Florida Institutional Animal Care and Use Committee. Rats were housed in an Assessment and Accreditation of Laboratory Animal Care (AAALAC)-accredited facility with a 12:12 light/dark cycle with *ad libitum* access to rodent chow and water. Adult female Sprague–Dawley rats (200–250 g, Harlan Laboratories, Indianapolis, IN, USA) were studied in two groups: SCI (left lateralized contusion injury, $n = 8$), and SCI + HBO ($n = 8$).

Surgical procedures

Anesthesia was induced with 3% isoflurane in O_2 and maintained at 2–3%. A dorsal midline incision was made from the second to fifth cervical segment and the C3-4 laminae were removed. A left lateralized contusion was induced using the Infinite Horizon impactor (Precision Systems & Instrumentation, Lexington, KY[22]). The impactor probe (2.5 mm diameter tip) was positioned between midline and the lateral edge of the spinal cord at C3/C4, and was raised 5 mm above the intact dura. The cord was contused at a pre-set force (200 kd, dwell time = 0). Overlying muscles were sutured with 4–0 Vicryl and the skin incision was closed using wound clips. Postsurgical care included buprenorphine at 12 h intervals (0.03 mg/kg, s.q.) for 48 h, lactated Ringers solution (5 mL/12 h, s.q.), and oral Nutri-cal supplements (1–3 mL/12 h, Webster Veterinary, MA, USA) until volitional drinking and eating resumed.

HBO treatment

HBO exposures began at 4 h after anesthesia recovery and continued daily for 10 days. Rats were placed in an HBO chamber (volume = 17 L; Hyperbaric Systems, Alexandria, VA, USA) that was sealed and flushed with 100% O_2. The chamber was pressurized over 6 min ($\sim$5 psi/min) until reaching 3.0 ATA. The pressure was maintained for 60 min, and the chamber was continually flushed with 100% O_2 (3 L/min). After the 60 min, the chamber was depressurized over 6 min. Body temperature was recorded immediately prior and following HBO.

Histology and immunochemistry

Rats were euthanized with intraperitoneal Beuthanasia® injection (150 mg/kg; Patterson Veterinary Supply, Alachua, FL, USA). Intracardial perfusion with ice-cold saline (500 mL) was followed by 4% paraformaldehyde (500 mL). The spinal cord was harvested and transferred to 30% sucrose in 1x phosphate buffered saline (PBS). The C2-6 spinal cord was longitudinally sectioned (20 μm) and slide mounted. For ionized calcium binding adaptor molecule 1 (Iba-1) immunostaining, a rabbit anti-Iba-1 (WAKO cat# 019-19741) was used at 1:400 dilution. Iba-1 can label microglia as well as filtrating macrophages, and accordingly, in the Results section we refer to cells simply as Iba-1 positive, rather than drawing a conclusion regarding the precise nature of the cells. For the neuronal marker, a mouse anti-NeuN antibody was used (1:1000; Encor Biotechnology, cat# MCA-1B7, Gainesville, FL, USA). Tissue sections were rehydrated in PBS prior to 95°C antigen retrieval in Trilogy solution (Cell Marque, Rocklin, CA, USA). Slides were blocked for endogenous peroxidase activity, serum blocked and incubated overnight with NeuN or Iba-1 antibodies, or isotype matched mouse immunoglobulin (negative control). Antibody binding was detected using the Elite HRP kit and ImmPACT DAB (Vector Labs, Burlingame, CA, USA). Following chromogenic development, slides were stained with rabbit anti-Iba-1 (1:400; Wako Chemicals, Richmond, VA, USA) and detected using a Vector Alkaline Phosphatase kit with Blue Alkaline Phosphatase Substrate. Positive control tissues and concentration matched immunoglobulin controls were included. For hematoxylin and eosin (H&E) staining, sections were cut, air dried to improve adherence, and then rehydrated in distilled water. Tissues were stained using standard H&E methodology (SelecTech staining system, Leica Biosystems).

Microscopy

Images were captured and quantified by a blinded investigator. An Olympus BX43 upright microscope and DP80 camera with CellSens software was used. Three cervical cord sections were imaged from each animal and included the dorsal horn (laminae 1-3), the lesion epicenter, and the ventral horn (laminae 7-9). Neurons and

microglia were quantified using custom-written MATLAB software (version 2019a, Natick, MA, USA; code available by request). Images were captured at 4x, loaded into MATLAB, and separated into individual color channels. A gray scale image was converted to a black and white image using a thresholding procedure (im2bw function). We then excluded items in the image <10 and 25 pixels for the microglia and neurons, respectively. Further, any item >1000 pixels was excluded. The remaining cell boundaries were counted, and average cell counts were calculated across the dorsal, epicenter, and ventral images.

Microarray analysis

Rats ($n = 4$/group) were injected intraperitoneally with Beuthanasia (150 mg/kg) solution. Cervical spinal tissues (C3-C5) were harvested, placed into RNA Later (Life Technologies, Carlsbad, CA, USA), and stored at -80°C. RNA extraction was performed using TRIzol, and isolated total RNA was purified using an RNeasy Mini kit (Qiagen, Valencia, CA, USA). The resulting quantity and purity of total RNA was tested through absorbance spectrophotometry at 230, 260, and 280 nm. RNA samples were sent to the Boston University Medical Center Microarray Core Facility for analysis using the Affymetrix Rat Gene Array 2.0ST. Raw Affymetrix CEL files were normalized to produce gene-level expression values using the Robust Multiarray Average (RMA)[23] in the *affy* package version 1.36.[24] included in the Bioconductor software suite (version 2.12[25]), and an Entrez Gene-specific probeset mapping (17.0.0) from the Molecular and Behavioral Neuroscience Institute (Brainarray) at the University of Michigan[26] (http://brainarray.mbni.med.umich.edu/Brainarray/Database/CustomCDF). Expression values were log2-transformed. Array quality was assessed by computing Relative Log Expression (RLE) and Normalized Unscaled Standard Error (NUSE) using the *affyPLM* Bioconductor package (version 1.34.0[27]). Principal component analysis (PCA) was performed using the *prcomp* R function with expression values that had been normalized across all samples to a mean of 0 and a standard deviation of 1. Pairwise differential gene expression was assessed by performing Student's *t* test on the coefficients of simple linear models created using the *lmFit* function in the *limma* package (version 3.14.4). Correction for multiple hypothesis testing was accomplished using the Benjamini–Hochberg false discovery rate (FDR).[28] Human homologs of rat genes were identified using HomoloGene (version 68[29]). Microarray analyses were performed using the R environment for statistical computing (version 2.15.1). Both .cel files and expression values were deposited into minimum information about a microarray experiment (MIAME) compliant NCBI Gene Expression Omnibus (GEO Series ID GSE185600).

A GSEA (version 2.2.1)[21] was used to identify biological pathways and processes that were coordinately up- or downregulated within each pairwise comparison. The Entrez Gene identifiers of the human homologs of the genes interrogated by the array were ranked according to the *t* statistic computed for each pairwise comparison. An enrichment score (ES) for each gene set measured the skewedness. Enrichment scores were then normalized (NES) by computing the ratio of the observed ES to the mean ES across 1000 random distributions of the members of the gene set across the ranked list. Because multiple comparisons were tested, we used the optimized FDR q value (FDR-q) with statistical significance set to ≤0.25.

RT-PCR

RNA extracted from cervical spinal tissue was used to examine genes of interest from the microarray analysis ($n = 4$/group for SCI and SCI+HBO); 2.4 μg RNA was reverse transcribed with the Superscript III First-Strand Synthesis System for RT-PCR (Thermo Fisher Scientific, Waltham, MA, USA), and 1 μL cDNA was added to a 24 μL PCR reaction using Taqman chemistry and the StepOnePlus RT-PCR system (Applied Biosystems, Foster City, CA, USA). Relative quantification of gene expression was performed using the comparative computed tomography method,[30] and values are expressed as fold difference relative to SCI. NFκB Inhibitor alpha (NFκBia; Rn01473557_g1), v-rel reticuloendotheliosis viral oncogene homolog A (RELA; Rn0150226_m1), Fas-associated via death domain (FADD; Rn00596168_m1), apoptotic peptidase activating factor 1 (APAF1; Rn00576832_m1), Caspase 9 (CASP9; Rn00581212_m1), slit homolog 2 (SLIT2; Rn00575268_m1), neurexin 1 (NRXN1; Rn00665869_m1), microtubule-associated protein tau (MAPT; Rn00691532_m1), leucine rich repeat containing 4C (LRRC4C; Rn01513938_m1), and netrin G1 (NTNG1; Rn01518579_m1) mRNA transcripts were assayed using pre-designed rat primer and probe sequences commercially available (Thermo Fisher Scientific). Glyceraldehyde-3-phosphate dehydrogenase (GAPDH; Rn01775763) was chosen as the reference gene based on evidence of unchanged expression with our experimental manipulations. Each data set was tested for equal variances followed by comparison between groups by unpaired *t* test. Significance was established at $p < 0.05$.

Results

Spinal cord histology

Spinal cord histological assessment was performed in a separate cohort of rats that were not used for the mRNA analyses ($n = 4$/group). Gross lesion pathology was evaluated after staining with H&E (Fig. 1). The spinal cord lesion epicenter was centered on the C4 spinal

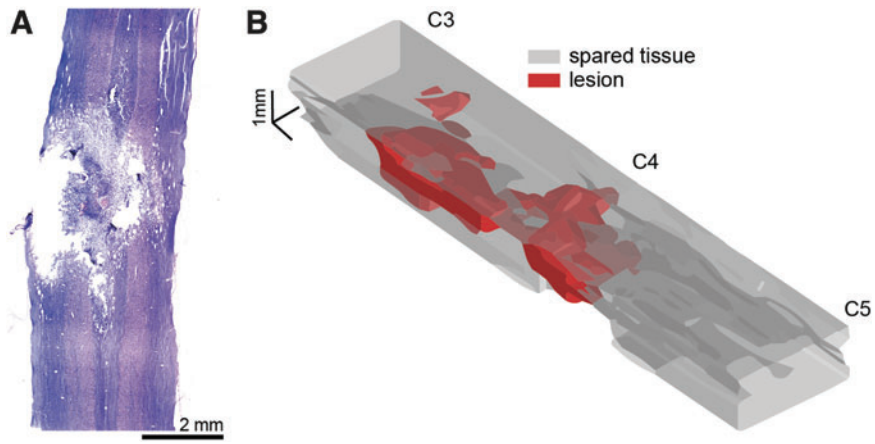

FIG. 1. Representative histological sections **(A)** and three-dimensional (3-D) reconstruction **(B)** of mid-cervical spinal cord contusion. Panel **A** shows a hematoxylin and eosin (H&E) stained longitudinal tissue section extending from ~ C3 to C5. Panel **B** shows a 3-D rendering that illustrates the spinal cord lesion. This image was created by tracing the lesion and spared tissue boundaries across nine longitudinal tissue sections, separated by 160 μm. The boundaries were interpolated to produce the 3-D image showing the estimated lesion and spared tissue volume. The lesion boundary interpolation is plotted in red, indicating areas in which histology confirmed a loss of tissue. The spared tissue boundaries were interpolated and plotted in gray. Color image is available online.

segment, with pathology extending both rostrally and caudally. The tissue damage typically extended across the spinal midline, reaching the contralateral dorsal and ventral gray matter shown in Figure 1.

Neurons were identified via immunostaining with a NeuN marker, and Iba-1 staining was used to visualize microglia (Fig. 2A, B). Tissue from HBO-treated rats showed an increase in the number of NeuN positive cells in the spinal cord ipsilateral to the contusion (Fig. 2C, $p=0.004$). A similar trend was seen in the contralateral spinal cord (Fig. 2D, $p=0.088$). The number of identified Iba-1 positive cells tended to be reduced in the ipsilesional spinal cord after HBO therapy ($p=0.168$, Fig. 2E), but there was no suggestion that HBO impacted the Iba-1 staining in the contralesional spinal cord ($p=0.851$, Fig. 2F). We also evaluated vacuolation in histological sections encompassing the spinal lesion (Fig. 2G, H). Although assessment of tissue vacuolation was not an *a priori* aim, we noticed an apparent impact of the HBO therapy and therefore quantified the vacuoles in the tissue. As shown in Figure 2I and J, there was a striking reduction in the extent of vacuolation in both the ipsilesional ($p=0.023$) and contralesional ($p=0.015$) spinal cord of HBO-treated rats.

Gene array pathway analyses

Spinal cord homogenates taken from C3-C5 (containing the lesion epicenter) were evaluated using an Affymetrix Rat Gene Array 2.0ST ($n=4$ SCI, $n=4$ SCI + HBO). The GSEA provided transcriptome-wide screening of gene sets that represent defined biological states or processes.[31] The ES, NES, and FDR for the top 10 statistically upregulated and downregulated pathways are presented in Tables 1 and 2, respectively. The primary theme that emerged from the upregulated pathways is ''aerobic metabolism'' (Table 1). Therefore, among the cellular processes associated with the upregulated pathways were electron transport, mitochondrial function, and oxidative phosphorylation. In regard to pathways that were downregulated after HBO treatment, the most striking observation was the prominence of pathways associated with inflammation (including cytokines and NF-κB) and apoptotic signaling (Table 2). Collectively, the GSEA analyses indicate that HBO treatment can alter the molecular signature of the lesioned spinal cord in a manner consistent with an anti-inflammatory and neuroprotective impact. We selected a few genes that the mRNA array analyses indicated were up- or downregulated by HBO exposure and evaluated changes in mRNA expression using rtPCR (Table S1 and Fig. S1). Most noteworthy, RT-PCR confirmed that mRNA expression of NF-κB ($p=0.032$) was decreased after HBO therapy.

Discussion

A growing body of work supports the hypothesis that HBO therapy can be beneficial after neurological injury, including stroke and SCI.[4,32,33] Building on this foundation, we found that daily, 1-h HBO therapy sessions (3.0

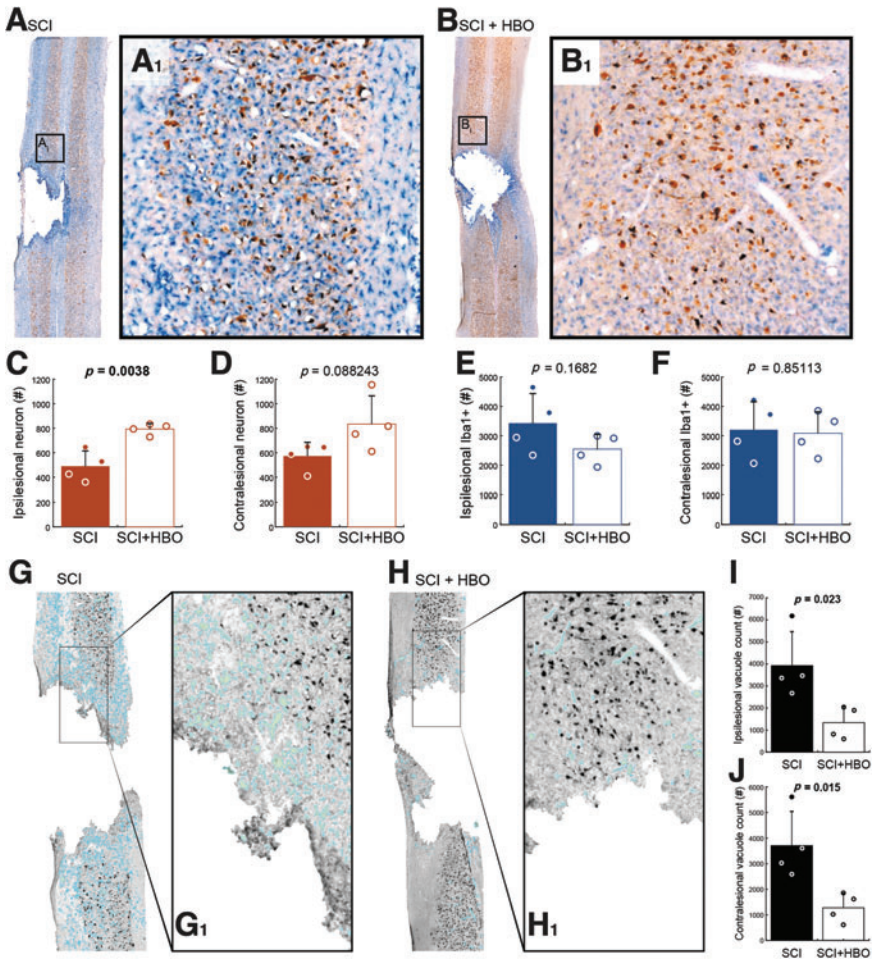

FIG. 2. Spinal cord histology indicates neuronal preservation and reduced tissue vacuolation after hyperbaric oxygen (HBO) treatment. Representative histological images containing the lesion epicenter are shown from an untreated rat **(A)**, and a rat that received HBO treatment **(B)**. These tissue sections were stained with NeuN (brown) and ionized calcium binding adaptor molecule 1 (Iba-1, blue). On average, more NeuN positive cells could be detected in the ipsilesional spinal card in HBO treated rats (**C**, $p = 0.0038$). A similar trend was noted in the contralesional spinal cord (**D**, $p = 0.0882$). Iba-positive counts were not statistically different between control and HBO-treated rats in the ipsilesional (**E**, $p = 0.1682$) or contralesional spinal cord (**F**, $p = 0.8511$). Panels **G** and **H** provide example histological sections that illustrate vacuolation. In these examples, the vacuoles in the tissue have been highlighted with light blue, and were identified using a custom MatLab script. Overall, there was a striking and statistically significant reduction in vacuolation in the ipsilesional (**I**, $p = 0.023$) and contralesional (**J**, $p = 0.015$) spinal cord after HBO treatment. Color image is available online.

ATA, 100% O_2), initiated on the day of SCI, can alter the molecular signature of the lesioned spinal cord in a manner consistent with an anti-inflammatory and neuroprotective impact.

HBO therapy after SCI

HBO is used commonly to treat decompression sickness or to aid peripheral wound healing. It has also been tested in multiple clinical trials related to brain injury and SCI.[4,32] Appropriate dosing of HBO is a paramount concern because oxygen toxicity and adverse effects are inevitable consequences at high ATA and/or sustained exposure. Oxygen toxicity results at least in part from oxidative stress and can produce loss of consciousness and generalized tonic-clonic seizures.[34] In the rat, seizures can occur if 3.0 ATA is sustained for 3–5 h. The time to seizure is reduced to between 5 and 90 min if the

Table 1. Top Ten Upregulated Pathways after HBO Therapy

MSig DB pathway name	*Size*	*ES*	*N-ES*	*FDR q*	*Comment*
REACTOME_TCA_CYCLE_AND_RESPIRATORY_ ELECTRON_TRANSPORT	104	0.518	2.305	0.001	The citric acid (TCA) cycle and respiratory electron transport; aerobic energy pathway
KEGG_CITRATE_CYCLE_TCA_CYCLE	29	0.675	2.301	0.001	TCA and Krebs cycle; aerobic energy pathway
REACTOME_RESPIRATORY_ELECTRON_TRANSPORT	57	0.581	2.259	0.001	Respiratory electron transport; aerobic energy pathway
REACTOME_RESPIRATORY_ELECTRON_TRANSPORT_ ATP_SYNTHESIS_BY_CHEMIOSMOTIC_COUPLING_AND_ HEAT_PRODUCTION_BY_UNCOUPLING_PROTEINS_	70	0.541	2.234	0.001	Respiratory electron transport, ATP synthesis by chemiosmotic coupling
REACTOME_GLUCOSE_METABOLISM	49	0.575	2.187	0.002	Glucose metabolism
MITOCHONDRIAL_INNER_MEMBRANE	55	0.539	2.122	0.007	The inner lipid bilayer of the mitochondrial envelope
MITOCHONDRIAL_MEMBRANE	73	0.513	2.111	0.007	Lipid bilayers that form the mitochondrial envelope
YGCANTGCR_UNKNOWN	110	0.465	2.077	0.010	Genes with ≥1 occurrence of the M96 YGCANTGCR motif in region spanning 4 kb at transcription start site
KEGG_PARKINSONS_DISEASE	96	0.481	2.070	0.010	Parkinson's disease
KEGG_OXIDATIVE_PHOSPHORYLATION	100	0.416	2.064	0.010	Oxidative phosphorylation

HBO, hyperbaric oxygen; MSig DB, Molecular Signatures Database; ES. enrichment score; N-ES, normalized enrichment score; FDR q, false discovery rate q-value; ATP,

hyperoxic gas is pressed to 5.0 ATA.[35] Note that ATA is ''absolute atmospheres,'' and, therefore, 1.0 ATA is equal to sea level barometric pressure.

For clinical efficacy, HBO therapy is thought to require 100% O_2 delivered at a minimum of 1.4 ATA and not exceeding 3.0 ATA.[34] Per a *New England Journal of Medicine* report, ''when used according to standard protocols, with oxygen pressures not exceeding 3 atmospheres and treatment sessions limited to a maximum of 120 minutes, hyperbaric therapy is safe.''[36] Therefore, HBO paradigms are designed to treat patients during the latent period of ''safe oxygen breathing,'' well before O_2 toxicity can develop. In a study of HBO therapy after traumatic brain injury in 48 human subjects (100% O_2, 2.4 ATA), the most commonly reported side effect was ear block (5.5% of patients). Incidence of seizures in patients treated with standard clinical HBO paradigms ($n > 80{,}000$) is reported at 0.002%.[37]

Here we used 1-h HBO exposures and chose 3.0 ATA as a ''high dose'' that is safe in short exposures. We

Table 2. Top Ten Downregulated Pathways after HBO Therapy

MSig DB pathway name	*Size*	*ES*	*N-ES*	*FDR q*	*Comment*
KEGG_LEISHMANIA_INFECTION	57	0.573	2.266	0.004	Associated with enhanced TGF-ß production and decreased cytokine induction such as IL12
BIOCARTA_NFKB_PATHWAY	22	0.712	2.255	0.003	NF-kß signaling pathway
BIOCARTA_CD40_PATHWAY	15	0.764	2.201	0.004	CD40-ligand signaling pathway; CD40 is a member of TNF receptor family
BIOCARTA_HIVNEF_PATHWAY	54	0.547	2.130	0.009	HIV-I Nef: negative effector of Fas and TNF; NEF interacts with apoptosis signal-regulating kinase
REACTOME_INTERFERON_GAMMA_SIGNALING	48	0.552	2.106	0.010	Interferon gamma signaling
BIOCARTA_TNFR2_PATHWAY	18	0.721	2.105	0.009	TNF receptor2 signaling pathway; TNFß is produced by activated lymphocytes and can be cytotoxic
HYDROLASE_ACTIVITY_HYDROLYZING_ O_GLYCOSYL_COMPOUNDS	35	0.600	2.094	0.009	Catalysis of the hydrolysis of any O-glycosyl bond
BIOCARTA_CHEMICAL_PATHWAY	22	0.655	2.062	0.012	Apoptotic signaling in response to DNA damage
REACTOME_NUCLEOTIDE_BINDING_DOMAIN_ LEUCINE_RICH_REPEAT_CONTAINING_ RECEPTOR_NLR_SIGNALING_PATHWAYS	40	0.565	2.048	0.013	Nucleotide-binding domain, leucine rich repeat containing receptor (NLR) signaling pathways
REACTOME_INNATE_IMMUNE_SYSTEM	190	0.424	2.036	0.015	Innate (non-specific) immune responses

HBO, hyperbaric oxygen; MSig DB, Molecular Signatures Database; ES, enrichment score; N-ES, normalized enrichment score; FDR q, false discovery rate q-value; TGF, transforming growth factor; IL, interleukin; NF, nuclear factor; TNF, tumor necrosis factor.

initiated HBO treatment on the day of SCI because the rationale for neuroprotection is strongest during this time frame when inflammatory and apoptotic processes are likely to be most active. The limited available data regarding post-injury therapeutic window suggests that early HBO exposure is critical,[38,39] and that repeated daily exposures may provide further benefit.[40]

A considerable number of pre-clinical studies in animal models are consistent with the hypothesis that HBO therapy can provide neuroprotection.[4] The earliest data, to our knowledge, are from 1976, with evidence that spinally injured sheep had improved motor recovery when HBO was applied 2 h after SCI.[11,12] Subsequent studies in animal models have reported that HBO therapy after SCI is associated with a reduction in spinal markers of oxidative stress including nitric oxide synthase,[13,14] upregulation of antioxidants,[41,42] reduced apoptosis,[15] and improved motor recovery.[17–19]

Here, we performed GSEA to identify molecular pathways that are impacted in the injured spinal cord following HBO treatment. We reasoned that GSEA would provide (1) an unbiased evaluation of the hypothesis that HBO therapy can impact the molecular response of the injured spinal cord, and (2) a hypothesis-generating data set for future mechanistic investigations of HBO after SCI. The GSEA showed that pathways broadly associated with aerobic metabolism (e.g., citric acid cycle, electron transport, mitochondria) showed a significant upregulation. This conclusion is bolstered by previous studies. For example, in a clinical trial, individuals with severe brain injury showed improved aerobic brain metabolism after acute HBO therapy.[43] Further, in an animal model of motor neuron disease, daily HBO can improve mitochondrial respiration in brain and spinal cord.[44] Another prominent finding of the GSEA was the downregulation of pathways associated with inflammation (e.g., cytokines and NF-κB) and apoptotic signaling. With regard to inflammation, a recent study in a rat SCI model reported that daily HBO therapy reduced spinal cord inflammation and suppressed NF-κB signaling.[20] Expression of NF-κB drives proinflammatory signaling genes including cytokines, chemokines, and adhesion molecules.[45] Our observation that gene expression pathways associated with neuronal death/loss were downregulated after HBO therapy is also supported by prior experimentation.[16,46]

The conclusions from the GSEA are supported by the histological outcomes of our study. In particular, we observed an increase in the neuronal cell counts in the injured spinal cord after HBO therapy. Further, we also noted that vacuolization of the histological sections was reduced after HBO. Vacuolization, a marker of white matter health, is associated with demyelination.[47] Further, a reduction in vacuolization has been reported to be a marker of neuroprotection.[48] Importantly, a previous research study of HBO therapy after SCI also reported a reduction of vacuolization in histological sections from the injured spinal cord.[13] Therefore, our histological data, combined with the molecular evaluation, contribute to the growing evidence that HBO therapy initiated after acute SCI can provide neuroprotection.

Conclusion

Before stating our conclusions, we acknowledge several caveats with regard to the current work. First, our study used only female rats, and the particular stage of the estrous cycle was an uncontrolled variable. Sex hormones can impact recovery after SCI,[49,50] and studying only female rats may have impacted the results, as could the particular phase of their estrous cycle at the time of injury. However, prior studies have indicated a benefit of HBO therapy in spinally injured male rats,[15,51] as well as in humans with SCI,[52,53] and, therefore, we do not think that the current results will be unique to females. We also acknowledge that our study had a relatively low sample size in each group. Some of the histological outcomes (e.g., contralesional neuronal counts, $p = 0.08$) tended to be impacted by HBO, but did not meet the 0.05 cutoff. This likely reflected the small sample size. Nevertheless, the current data indicate that HBO therapy, initiated shortly after SCI and continued for 10 days, can alter the molecular signature of the injured spinal cord in a manner consistent with an anti-inflammatory and neuroprotective impact. This conclusion is supported by the mRNA GSEA, spinal cord histology, and prior publications on this topic.

Acknowledgments

We thank Marda Jorgenson for her expert help conducting the histological and immunochemical procedures. We thank Dr. Nicole Tester for assistance with surgical procedures. In addition, we are grateful to Nichole Gregory, Aaron K. Hoyt, and Cassandra Schuster for assisting with post-surgical procedures and aspects of the tissue processing.

Funding Information

Funding was provided by Craig H. Neilsen Foundation grants 313369 (S.M.F.T.), F31 HL145831 (M.D.S.), and 5R01HL153140-02 (D.D.F.). The Boston University Microarray and Sequencing Resource Core Facility performed the gene array experiments.

Author Disclosure Statement

No competing financial interests exist.

Supplementary Material

Supplementary Figure S1
Supplementary Table S1

References

1. Harch, P.G. (2015). Hyperbaric oxygen in chronic traumatic brain injury: oxygen, pressure, and gene therapy. Med. Gas Res. 5, 9.
2. Figueroa, X.A., and Wright, J.K. (2016). Hyperbaric oxygen: B-level evidence in mild traumatic brain injury clinical trials. Neurology 87, 1400–1406.
3. Mozayeni, B.R., Duncan, W., Zant, E., Love, T.L., Beckman, R.L., and Stoller, K.P. (2019). The National Brain Injury Rescue and Rehabilitation Study – a multicenter observational study of hyperbaric oxygen for mild traumatic brain injury with post-concussive symptoms. Med. Gas Res. 9, 1–12.
4. Patel, N.P., and Huang, J.H. (2017). Hyperbaric oxygen therapy of spinal cord injury. Med. Gas Res. 7, 133–143.
5. Hilton, B.J., Moulson, A.J., and Tetzlaff, W. (2017). Neuroprotection and secondary damage following spinal cord injury: concepts and methods. Neurosci. Lett. 652, 3–10.
6. Emery, E., Aldana, P., Bunge, M.B., Puckett, W., Srinivasan, A., Keane, R.W., Bethea, J., and Levi, A.D. (1998). Apoptosis after traumatic human spinal cord injury. J. Neurosurg. 89, 911–920.
7. Crowe, M.J., Bresnahan, J.C., Shuman, S.L., Masters, J.N., and Beattie, M.S. (1997). Apoptosis and delayed degeneration after spinal cord injury in rats and monkeys. Nat. Med. 3, 73–76.
8. Bunge, R.P., Puckett, W.R., Becerra, J.L., Marcillo, A., and Quencer, R.M. (1993). Observations on the pathology of human spinal cord injury. A review and classification of 22 new cases with details from a case of chronic cord compression with extensive focal demyelination. Adv. Neurol. 59, 75–89.
9. Kelly, D.L., Jr., Lassiter, K.R., Calogero, J.A., and Alexander, E., Jr. (1970). Effects of local hypothermia and tissue oxygen studies in experimental paraplegia. J. Neurosurg. 33, 554–563.
10. Kelly, D.L., Jr., Lassiter, K.R., Vongsvivut, A., and Smith, J.M. (1972). Effects of hyperbaric oxygenation and tissue oxygen studies in experimental paraplegia. J. Neurosurg. 36, 425–429.
11. Yeo, J.D., McKenzie, B., Hindwood, B., and Kidman, A. (1976). Treatment of paraplegic sheep with hyperbaric oxygen. Med. J. Aust. 1, 538–540.
12. Yeo, J.D., Stabback, S., and McKenzie, B. (1977). A study of the effects of hyperbaric oxygen on the experimental spinal cord injury. Med. J. Aust. 2, 145–147.
13. Huang, H., Xue, L., Zhang, X., Weng, Q., Chen, H., Gu, J., Ye, S., Chen, X., Zhang, W., and Liao, H. (2013). Hyperbaric oxygen therapy provides neuroprotection following spinal cord injury in a rat model. Int. J. Clin. Exp. Pathol. 6, 1337–1342.
14. Dayan, K., Keser, A., Konyalioglu, S., Erturk, M., Aydin, F., Sengul, G., and Dagci, T. (2012). The effect of hyperbaric oxygen on neuroregeneration following acute thoracic spinal cord injury. Life Sci. 90, 360–364.
15. Ying, X., Tu, W., Li, S., Wu, Q., Chen, X., Zhou, Y., Hu, J., Yang, G., and Jiang, S. (2019). Hyperbaric oxygen therapy reduces apoptosis and dendritic/synaptic degeneration via the BDNF/TrkB signaling pathways in SCI rats. Life Sci. 229, 187–199.
16. Long, Y., Liang, F., Gao, C., Li, Z., and Yang, J. (2014). Hyperbaric oxygen therapy reduces apoptosis after spinal cord injury in rats. Int. J. Clin. Exp. Med. 7, 4073–4081.
17. Wang, Y., Li, C., Gao, C., Li, Z., Yang, J., Liu, X., and Liang, F. (2016). Effects of hyperbaric oxygen therapy on RAGE and MCP-1 expression in rats with spinal cord injury. Mol. Med. Rep. 14, 5619–5625.
18. Sun, Y., Liu, D., Su, P., Lin, F., and Tang, Q. (2016). Changes in autophagy in rats after spinal cord injury and the effect of hyperbaric oxygen on autophagy. Neurosci. Lett. 618, 139–145.
19. Wang, Y., Zhang, S., Luo, M., and Li, Y. (2014). Hyperbaric oxygen therapy improves local microenvironment after spinal cord injury. Neural Regen. Res. 9, 2182–2188.
20. Zhou, Y., Dong, Q., Pan, Z., Song, Y., Su, P., Niu, Y., Sun, Y., and Liu, D. (2019). Hyperbaric oxygen improves functional recovery of the injured spinal cord by inhibiting inflammation and glial scar formation. Am. J. Phys. Med. Rehabil. 98, 914–920.
21. Subramanian, A., Tamayo, P., Mootha, V.K., Mukherjee, S., Ebert, B.L., Gillette, M.A., Paulovich, A., Pomeroy, S.L., Golub, T.R., Lander, E.S., and Mesirov, J.P. (2005). Gene set enrichment analysis: a knowledge-based approach for interpreting genome-wide expression profiles. Proc. Natl. Acad. Sci. U. S. A. 102, 15,545–15,550.
22. Scheff, S.W., Rabchevsky, A.G., Fugaccia, I., Main, J.A., and Lumpp, J.E. (2003). Experimental modeling of spinal cord injury: characterization of a force-defined injury device. J. Neurotrauma 20, 179–193.
23. Irizarry, R.A., Hobbs, B., Collin, F., Beazer-Barclay, Y.D., Antonellis, K.J., Scherf, U., and Speed, T.P. (2003). Exploration, normalization, and summaries of high density oligonucleotide array probe level data. Biostatistics 4, 249–264.
24. Gautier, L., Cope, L., Bolstad, B.M., and Irizarry, R.A. (2004). affy-–analysis of Affymetrix GeneChip data at the probe level. Bioinformatics 20, 307–315.
25. Gentleman, R.C., Carey, V.J., Bates, D.M., Bolstad, B., Dettling, M., Dudoit, S., Ellis, B., Gautier, L., Ge, Y., Gentry, J., Hornik, K., Hothorn, T., Huber, W., Iacus, S., Irizarry, R., Leisch, F., Li, C., Maechler, M., Rossini, A.J., Sawitzki, G., Smith, C., Smyth, G., Tierney, L., Yang, J.Y., and Zhang, J. (2004). Bioconductor: open software development for computational biology and bioinformatics. Genome Biol. 5, R80.
26. Dai, M., Wang, P., Boyd, A.D., Kostov, G., Athey, B., Jones, E.G., Bunney, W.E., Myers, R.M., Speed, T.P., Akil, H., Watson, S.J., and Meng, F. (2005). Evolving gene/transcript definitions significantly alter the interpretation of GeneChip data. Nucleic Acids Res. 33, e175.
27. Brettschneider, J., Collin, F., Bolstad, B.M., and Speed, T.P. (2008). Quality assessment for short oligonucleotide microarray data. Technomet. 50, 241–264.
28. Benjamini, Y., and Hochberg, Y. (1995). Controlling the false discovery rate: a practical and powerful approach to multiple testing. J. R. Stat. Soc. Series B Stat. Methodol. 57, 289–300.
29. NCBI Research Coordinators (2013). Database resources of the National Center for Biotechnology Information. Nucleic Acids Res. 41, D8–D20.
30. Schmittgen, T.D., and Livak, K.J. (2008). Analyzing real-time PCR data by the comparative C(T) method. Nat. Protoc. 3, 1101–1108.
31. Liberzon, A., Birger, C., Thorvaldsdottir, H., Ghandi, M., Mesirov, J.P., and Tamayo, P. (2015). The Molecular Signatures Database (MSigDB) hallmark gene set collection. Cell Syst. 1, 417–425.
32. Falavigna, A., Teles, A.R., Velho, M.C., and Kleber, F.D. (2009). Effects of hyperbaric oxygen therapy after spinal cord injury: systematic review. Coluna/Columna 8, 330–336.
33. Ding, Z., Tong, W.C., Lu, X.X., and Peng, H.P. (2014). Hyperbaric oxygen therapy in acute ischemic stroke: a review. Interv. Neurol. 2, 201–211.
34. Ciarlone, G.E., Hinojo, C.M., Stavitzski, N.M., and Dean, J.B. (2019). CNS function and dysfunction during exposure to hyperbaric oxygen in operational and clinical settings. Redox Biol. 27, 101159.
35. Simon, A.J., and Torbati, D. (1982). Effects of hyperbaric oxygen on heart, brain, and lung functions in rat. Undersea Biomed. Res. 9, 263–275.
36. Tibbles, P.M., and Edelsberg, J.S. (1996). Hyperbaric-oxygen therapy. N. Engl. J. Med. 334, 1642–1648.
37. Yildiz, S., Aktas, S., Cimsit, M., Ay, H., and Togrol, E. (2004). Seizure incidence in 80,000 patient treatments with hyperbaric oxygen. Aviat. Space Environ. Med. 75, 992–994.
38. Higgins, A.C., Pearlstein, R.D., Mullen, J.B., and Nashold, B.S., Jr. (1981). Effects of hyperbaric oxygen therapy on long-tract neuronal conduction in the acute phase of spinal cord injury. J. Neurosurg. 55, 501–510.
39. Murakami, N., Horinouchi, T., Sakurai, M., ENjima, Y., Matsukawa, S., Kato, M., and Tabayashi, K. (2001). Hyperbaric oxygen therapy given 30 minutes after spinal cord ischemia attenuates selective motor neuron death in rabbits. Crit. Care Med. 29, 814–818.
40. Huang, L., Mehta, M.P., Nanda, A., and Zhang, J.H. (2003). The role of multiple hyperbaric oxygenation in expanding therapeutic windows after acute spinal cord injury in rats. J. Neurosurg. 99, 198–205.
41. Kahraman, S., Duz, B., Kayali, H., Korkmaz, A., Oter, S., Aydin, A., and Sayal, A. (2007). Effects of methylprednisolone and hyperbaric oxygen on oxidative status after experimental spinal cord injury: a comparative study in rats. Neurochem. Res. 32, 1547–1551.
42. Wang, L., Li, W., Kang, Z., Liu, Y., Deng, X., Tao, H., Xu, W., Li, R., Sun, X., and Zhang, J.H. (2009). Hyperbaric oxygen preconditioning attenuates early apoptosis after spinal cord ischemia in rats. J. Neurotrauma 26, 55–66.
43. Rockswold, S.B., Rockswold, G.L., Vargo, J.M., Erickson, C.A., Sutton, R.L., Bergman, T.A., and Biros, M.H. (2001). Effects of hyperbaric oxygenation therapy on cerebral metabolism and intracranial pressure in severely brain injured patients. J. Neurosurg. 94, 403–411.
44. Dave, K.R., Prado, R., Busto, R., Raval, A.P., Bradley, W.G., Torbati, D., and Perez-Pinzon, M.A. (2003). Hyperbaric oxygen therapy protects against mitochondrial dysfunction and delays onset of motor neuron disease in Wobbler mice. Neuroscience 120, 113–120.
45. Wang, Y., Mao, L., Zhang, L., Zhang, L., Yang, M., Zhang, Z., Li, D., Fan, C., and Sun, B. (2016). Adoptive regulatory T-cell therapy attenuates subarachnoid hemorrhage-induced cerebral inflammation by suppressing TLR4/NF-B signaling oathway. Curr. Neurovasc. Res. 13, 121–126.
46. Shams, Z., Khalatbary, A.R., Ahmadvand, H., Zare, Z., and Kian, K. (2017). Neuroprotective effects of hyperbaric oxygen (HBO) therapy on neuronal death induced by sciatic nerve transection in rat. BMC Neurol. 17, 220.

47. Duncan, I.D., Brower, A., Kondo, Y., Curlee, J.F., Jr., and Schultz, R.D. (2009). Extensive remyelination of the CNS leads to functional recovery. Proc. Natl. Acad. Sci. U. S. A. 106, 6832–6836.
48. Saito, T., Saito, S., Yamamoto, H., and Tsuchida, M. (2013). Neuroprotection following mild hypothermia after spinal cord ischemia in rats. J. Vasc. Surg. 57, 173–181.
49. Doperalski, N.J., Sandhu, M.S., Bavis, R.W., Reier, P.J., and Fuller, D.D. (2008). Ventilation and phrenic output following high cervical spinal hemisection in male vs. female rats. Respir. Physiol. Neurobiol. 162, 160–167.
50. Raghava, N., Das, B.C., and Ray, S.K. (2017). Neuroprotective effects of estrogen in CNS injuries: insights from animal models. Neurosci. Neuroecon. 6, 15–29.
51. Zhao, Y., Zheng, Y., Xiao, Z., Liu, J., Yang, L., Liu, F., and Cao, D. (2020). Diffusion tensor imaging in the evaluation of the long-term efficacy of HBO2 therapy in rats after traumatic spinal cord injury. Undersea Hyperb. Med. 47, 435–443.
52. Sun, L., Zhao, L., Li, P., Liu, X., Liang, F., Jiang, Y., Kang, N., Gao, C., and Yang, J. (2019). Effect of hyperbaric oxygen therapy on HMGB1/NF-kappaB expression and prognosis of acute spinal cord injury: a randomized clinical trial. Neurosci. Lett. 692, 47–52.
53. Huang, L., Zhang, Q., Fu, C., Liang, Z., Xiong, F., He, C., and Wei, Q. (2021). Effects of hyperbaric oxygen therapy on patients with spinal cord injury: a systematic review and meta-analysis of randomized controlled trials. J. Back Musculoskelet. Rehabil. 34, 905–913.